Identification and assessment of *FN1*, *MET*, *KRT19* and *CLDN1* as key dysregulated genes in papillary thyroid cancer through transcriptomic profiling and expression analysis

ANETTE ROXANA GASTELUM-QUIROZ[1,2*], NOEMÍ GARCÍA-MAGALLANES[2*], ANDREA ROSS-OROZCO[1,2], MARCO ALVAREZ-ARRAZOLA[2,3], FRED LUQUE-ORTEGA[4], KARLA LIZBETH MORALES-HERNÁNDEZ[1,5], DORA CEDANO-PRIETO[6], VANESSA G. FÉLIX[7] and ELIAKYM ARÁMBULA-MERAZ[1,6]

[1]Department of Postgraduate Biomedical Sciences, Faculty of Chemical-Biological Sciences, Autonomous University of Sinaloa, 80010 Culiacán, Sinaloa, México; [2]Laboratory of Biomedicine and Molecular Biology, Department of Biotechnology Engineering, Polytechnic University of Sinaloa, 82199 Mazatlán, Sinaloa, México; [3]Alvarez & Arrazola Radiologists, 82140 Mazatlán, Sinaloa, Mexico; [4]Basic Sciences Laboratory, Faculty of Dentistry, Autonomous University of Sinaloa, 80010 Culiacán, Sinaloa, México; [5]Department of Biomedical Sciences, Autonomous University of The West, 82100 Mazatlán, Sinaloa, México; [6]Laboratory of Genetics and Molecular Biology, Faculty of Chemical and Biological Sciences, Autonomous University of Sinaloa, 80010 Culiacan, Sinaloa, México; [7]Academic Unit of Information Technology and Digital Innovation, Polytechnic University of Sinaloa, 82199 Mazatlán, Sinaloa, México

Received January 16, 2026; Accepted July 30, 2026

DOI: 10.3892/ol.2026.15854

Abstract. Papillary thyroid carcinoma (PTC) is the most common type of endocrine malignancy worldwide. Although the prognosis of PTC is generally favorable, understanding its molecular mechanisms is of great importance for improving diagnostic stratification and clinical management. The present study aimed to identify genes that are consistently differentially expressed in PTC through an integrative analysis of transcriptomic datasets combined with experimental validation. Differential expression analysis of six RNA-sequencing datasets comparing PTC and adjacent non-tumor tissue identified 131 commonly dysregulated genes, including 128 upregulated and 3 downregulated genes. Functional enrichment and Kyoto Encyclopedia of Genes and Genomes analyses revealed that the aforementioned differentially expressed genes were significantly associated with 'tissue development', 'cell adhesion' and 'plasma membrane organization'. Additionally, protein-protein interaction network and centrality analyses identified fibronectin 1 (*FN1*), MET proto-oncogene, receptor tyrosine kinase (*MET*), keratin 19 (*KRT19*) and claudin 1 (*CLDN1*) as hub genes consistently ranked among the top candidates. The mRNA expression levels of these genes were detected in an independent cohort of 86 patients, including 42 with PTC and 44 with a benign thyroid nodule (BTN), by reverse transcription-quantitative PCR. Furthermore, *in silico* analysis was performed using data from the Human Protein Atlas. The results demonstrated that all 4 genes were significantly upregulated in PTC tissues compared with those in BTN tissues ($P<0.001$). Collectively, these findings support the presence of a reproducible transcriptomic pattern in PTC. Furthermore, *FN1*, *MET*, *KRT19* and *CLDN1* were identified as robust candidate biomarkers that warrant further functional characterization and clinical evaluation.

Introduction

Thyroid cancer is the most common endocrine malignancy worldwide, while papillary thyroid carcinoma (PTC) accounts for ~80% of all cases (1,2). Although PTC generally carries a favorable prognosis, its global incidence has increased steadily in recent decades. This trend underscores the need to improve our understanding of the molecular mechanisms underlying PTC pathogenesis to optimize diagnostic approaches, refine risk stratification and guide therapeutic strategies (3).

Several genetic alterations have been well described in PTC, including the *BRAFV600E* mutation and mutations in the RAS family genes (*NRAS*, *KRAS* and *HRAS*) (4). However, these alterations alone cannot fully explain the heterogeneous clinical behavior observed in patients with this disease. The 2025 American Thyroid Association Management Guidelines for Adult Patients with Differentiated Thyroid

Correspondence to: Dr Eliakym Arámbula-Meraz, Laboratory of Genetics and Molecular Biology, Faculty of Chemical and Biological Sciences, Autonomous University of Sinaloa, University City, Américas Avenue and Josefa Ortiz de Domínguez, 80010 Culiacán, Sinaloa, Mexico
E-mail: eliakymarambula@uas.edu.mx

*Contributed equally

Key words: papillary thyroid cancer, transcriptomic profiling, RNA-sequencing, gene expression

Cancer emphasize the importance of expanding the molecular framework of thyroid carcinogenesis, including the integration of transcriptomic approaches capable of capturing broader patterns of gene dysregulation (5).

Transcriptomic analysis can enable the simultaneous evaluation of thousands of genes, thus facilitating the identification of differentially expressed genes (DEGs) with potential diagnostic, prognostic and therapeutic potential. RNA-sequencing (RNA-seq) has become the standard technology for gene expression profiling, as it offers greater sensitivity, a wider dynamic range and the ability to detect novel transcripts compared with microarray-based approaches (6). Despite these advantages, several PTC transcriptomic studies have relied on microarray data or single-cohort analyses, commonly restricted to The Cancer Genome Atlas (TCGA) (7-18). Consequently, comprehensive analyses integrating multiple independent RNA-seq datasets that are validated in external cohorts remain limited. Furthermore, despite the increasing number of PTC transcriptomic studies, considerable variability has been reported across datasets in the genes identified as differentially expressed (7-9). This heterogeneity can hamper the establishment of a consistent molecular framework that can be reliably translated into clinical practice. Identifying genes that are consistently dysregulated across independent cohorts is therefore essential for defining robust molecular characteristics of PTC beyond dataset-specific findings.

Although our previous study identified *KRT19* and *CLDN1* as dysregulated genes in thyroid cancer, the reproducibility of these findings across independent transcriptomic datasets and different populations, as well as the identification of additional robust candidate biomarkers, remained to be established. Therefore, the present study aimed to identify genes consistently dysregulated in PTC across independent transcriptomic datasets and to evaluate their expression in clinically relevant thyroid nodule samples, thus strengthening the biological significance and potential diagnostic relevance of a reproducible molecular signature of PTC.

Materials and methods

RNA-seq data acquisition. RNA-seq datasets were retrieved from the NCBI Gene Expression Omnibus (GEO) repository (https://www.ncbi.nlm.nih.gov/geo/) (19) to identify dysregulated genes in PTC through differential expression analysis. The database search was performed using the key word 'papillary thyroid carcinoma' with the following filters applied: Organism (*Homo sapiens*), study type (expression profiling by high-throughput sequencing) and entry type (datasets). Studies were eligible if they contained RNA-seq data derived from thyroid tissue samples obtained from patients with histologically confirmed PTC, along with either adjacent non-tumoral thyroid tissues or benign thyroid nodules (BTNs) from independent patients without cancer, which served as controls. Only datasets providing accessible raw read count matrices were included. Datasets based on microarray platforms, non-human samples or cell lines were excluded. A total of six datasets, namely GSE87410, GSE153659, GSE171011, GSE197443, GSE165724 and GSE201365 (20-24), met the predefined inclusion criteria and were included in the downstream analyses. A detailed summary of the included GEO datasets, including sample size, control type, year of publication and sequencing platform information, is provided in Table SI.

Data preprocessing. To reduce potential bias from low-count genes associated with low sequencing depth, filtering was performed prior to differential expression analysis. Specifically, genes with a total read count of <10 across all samples within each dataset were removed. No additional per-sample minimum count threshold was applied. All preprocessing steps were performed using the dplyr package (version 1.1.4; https://dplyr.tidyverse.org/) in R statistical software (version 4.4.1; https://www.r-project.org/).

Identification of DEGs. Differential expression analysis was performed using the DESeq2 package (version 1.34.1) (25). Genes with an adjusted $P<0.05$ were considered significantly differentially expressed. In addition, to identify genes with biologically meaningful expression differences, an additional threshold of absolute $\log_2$ fold change ($|log2FC|>2$) was applied.

Functional enrichment and Kyoto Encyclopedia of Genes and Genomes (KEGG) pathway analysis. Functional enrichment analyses were performed to evaluate the biological significance of the identified DEGs. An adjusted P-value of <0.05 was considered significantly enriched and top 10 enriched terms were selected for each category. Gene Ontology (GO) enrichment and KEGG pathway analyses of the candidate DEGs were conducted using the R package, clusterProfiler (version 4.6.2) (26-28).

Construction of the protein-protein interaction (PPI) network and identification of hub genes. The PPI network of the identified DEGs was constructed using Search Tool for the Retrieval of Interacting Genes/Proteins (STRING; version 12.0), with an interaction score cut-off of >0.4 (29). The resulting network was imported into Cytoscape (version 3.10.2) (30) for visualization and further analysis. Hub genes were identified using the CytoHubba plugin by applying multiple centrality algorithms, including Maximum Neighborhood Component, degree, closeness, radiality, Maximal Clique Centrality and Edge Percolated Component, to rank genes with the highest connectivity and potential biological relevance in PTC (31).

Experimental validation of hub genes by reverse transcription-quantitative PCR (RT-qPCR). To validate hub gene expression, a cross-sectional analytical study was conducted, which included 86 samples obtained from patients attending the diagnostic radiology center, Alvarez & Arrazola Radiologists (Mazatlán, México) between February 2022 and August 2024. Patients with suspicious findings on thyroid ultrasound were consecutively recruited and subsequently underwent ultrasound-guided fine needle aspiration (FNA) biopsy for cytological assessment. To minimize interobserver variability, all cytological evaluations were performed by a single experienced pathologist. Cytological classification was performed according to the 2017 Bethesda System for Reporting Thyroid Cytopathology (32). For the present study, only patients ≥18 years of age with definitive cytological classification were included in the analysis. Specifically, cases

categorized as Bethesda II were assigned to the BTN group, while cases classified as Bethesda V and VI comprised the PTC group. These categories were selected due to their higher level of diagnostic certainty in distinguishing benign from malignant lesions. Cases with non-diagnostic samples (Bethesda I), indeterminate cytology (Bethesda III or IV) or incomplete clinical data were excluded to reduce the risk of misclassification bias. Samples with insufficient quality or integrity, as well as cases in which patients voluntarily withdrew, were also excluded. Histopathological confirmation following surgical resection was not available and is acknowledged as a limitation of the present study. The study protocol was approved by the Ethics and Research Committee of the Polytechnic University of Sinaloa (Mazatlán, México; approval no. 001-2022-CEI), and all participants provided written informed consent forms prior to sample collection. The cohort included in the present study was independent from previously published cohorts. Samples were preserved in RNA Protect Cell Reagent solution (Qiagen GmbH) and subsequently processed and analyzed at the Laboratory of Biomedicine and Molecular Biology at the Polytechnic University of Sinaloa.

RT-qPCR analysis. Total RNA was extracted using the RNeasy Plus Micro Kit (Qiagen GmbH) according to the manufacturer's instructions. cDNA was synthesized using the GoTaq 2-step RT-qPCR system Probe kit (Promega Corporation) according to the manufacturer's instructions. Reverse transcription was carried out under the following thermal conditions: 5 min at 25˚C, 45 min at 42˚C and 15 min at 70˚C. qPCR was performed using PrimeTime™ qPCR Probes [claudin 1 (*CLDN1*), Hs.PT.58.15247281; keratin 19 (*KRT19*), Hs.PT.58.4188708; fibronectin 1 (*FN1*), Hs.PT.58.40005963; and MET proto-oncogene, receptor tyrosine kinase (*MET*), Hs.PT.58.339430] and PrimeTime™ Gene Expression Master Mix (Integrated DNA Technologies, Inc.) on a StepOnePlus real-time thermocycler (Applied Biosystems; Thermo Fisher Scientific, Inc.). The amplification conditions consisted of an initial denaturation at 95˚C for 10 min, followed by 40 cycles of denaturation at 95˚C for 10 sec and annealing/extension at 60˚C for 20 sec. β-actin (Hs.PT.39a.22214847) served as the endogenous control. Relative gene expression levels were calculated using the previously described $2^{-\Delta\Delta Cq}$ method (33). Statistical analyses were carried out to evaluate significant differences in gene expression between the PTC and BTN groups.

In silico validation of hub gene expression at the protein level. To further assess whether mRNA expression patterns were consistent with protein abundance, hub gene expression was evaluated *in silico* using immunohistochemistry (IHC) data available from the Human Protein Atlas (https://www.proteinatlas.org/) (34). Representative IHC images of normal thyroid tissue and PTC samples were retrieved and qualitatively compared.

Statistical analysis. All experiments were performed in duplicate. Descriptive statistics were applied to qualitative variables, which are presented as frequencies and percentages, and to quantitative variables, which are expressed as mean ± SD. Associations between qualitative variables were assessed using the χ^2 or Fisher's exact test, as appropriate. Differences between two groups were analyzed using unpaired Student's t-test or the Mann-Whitney U test according to the results of the Shapiro-Wilk normality test. $P<0.05$ was considered to indicate a statistically significant difference. Statistical analyses were performed using SPSS (version 25.0; IBM Corp.).

Results

Identified DEGs. Differential expression analysis was performed independently for each of the six datasets (Fig. 1). Across all datasets, a total of 131 genes were consistently dysregulated, including 128 upregulated and 3 downregulated genes (Fig. 2). These genes were included in subsequent functional enrichment and PPI network analyses.

Functional enrichment and KEGG pathway analysis. Functional enrichment analysis of the common DEGs revealed significant overrepresentation of GO terms related to biological processes (BP) and cellular components (CC), whereas no significant enrichment was observed for molecular function (Fig. 3A and B). Within the BP category, the most significantly enriched GO terms included 'animal organ development' (GO:0048513), 'tissue development' (GO:0009888) and 'cell adhesion' (GO:0007155), which encompassed the largest number of DEGs. In the CC category, enriched terms were primarily associated with plasma membrane organization and intercellular junction structures, including 'cell junction' (GO:0030054), 'integral component of plasma membrane' (GO:0005887), 'anchoring junction' (GO:0070161) and 'intrinsic component of plasma membrane' (GO:0031226). The GO enrichment results, including BP and CC categories, are listed in Tables SII and SIII. The aforementioned findings suggest that the dysregulated genes in PTC were primarily involved in pathways governing cell adhesion and tissue integrity, indicating potential alterations in intercellular communication and plasma membrane organization in tumor cells. KEGG pathway analysis further supported these observations, highlighting enrichment in cancer-related and cell adhesion pathways, including 'small cell lung cancer' (hsa05222), 'cell adhesion molecules' (hsa04514), 'cornified envelope formation' (hsa04382) and 'virion-hepatitis viruses' (hsa03272) (Fig. 3C). The complete KEGG enrichment results are provided in Table SIV.

Identification of hub genes. The PPI network constructed from the 131 common DEGs is presented in Fig. 4. Hub genes were identified using the CytoHubba plugin in Cytoscape (version 3.10.2), applying six centrality algorithms. Only genes consistently ranked among the top candidates across all six methods were selected as hub genes (Table I). This integrative network-based approach enabled the identification of nodes with high topological centrality, reflecting strong connectivity and potential biological influence within the interaction network. A total of 4 genes, namely *FN1*, *MET*, *KRT19* and *CLDN1*, were selected through an intersection-based strategy, in which only genes shared among the top-ranked candidates identified by all six centrality metrics were retained, supporting their relevance within the PPI network and their potential involvement in key biological processes associated with PTC. The expression profile of

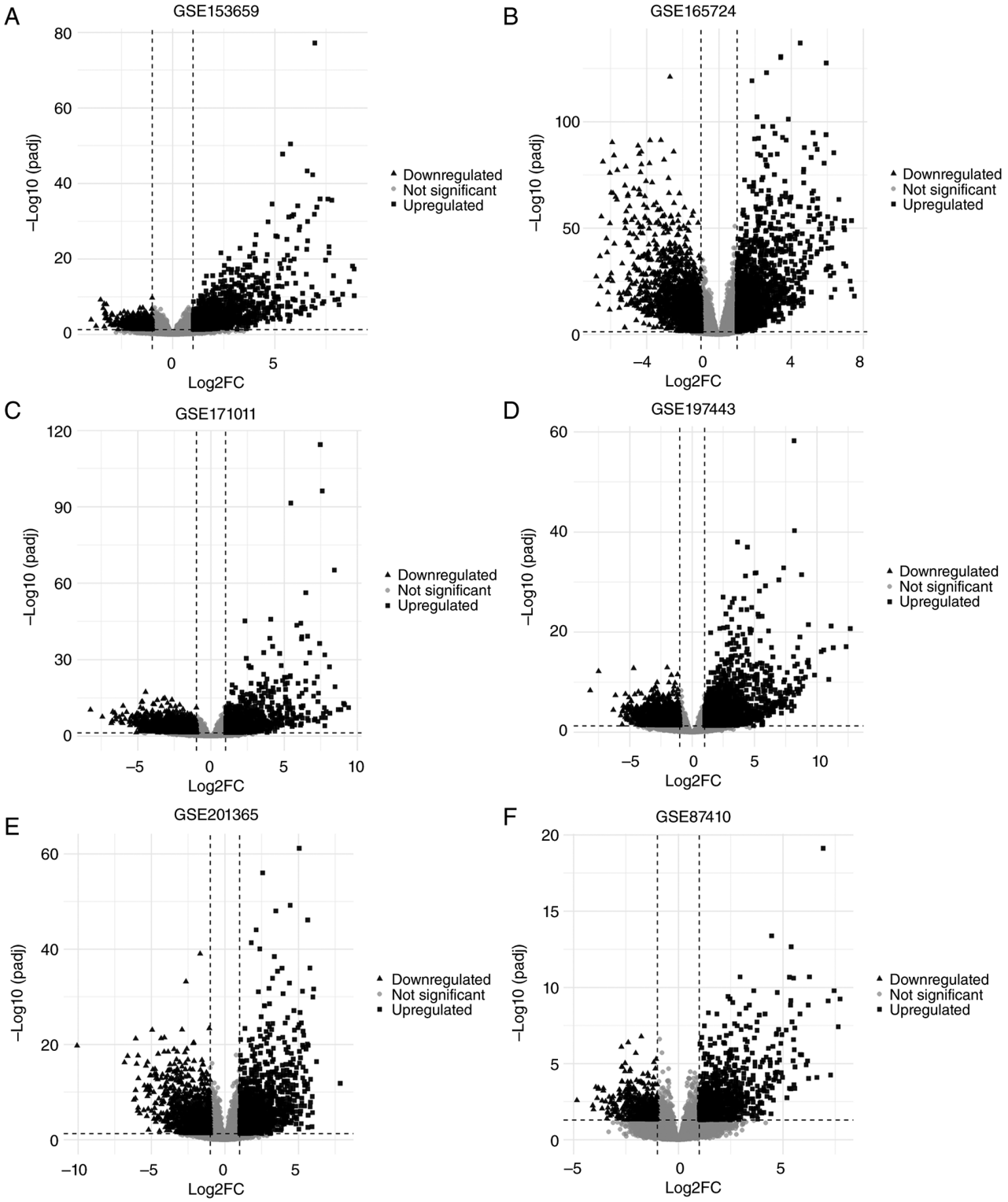

Figure 1. Volcano plots of differential gene expression analyses from six independent PTC datasets. Each panel represents one dataset comparing PTC samples with benign or normal thyroid tissue: (A) GSE153659, (B) GSE165724, (C) GSE171011, (D) GSE197443, (E) GSE201365 and (F) GSE87410. The x-axis shows the log2FC, while the y-axis represents statistical significance [-log10(padj)]. Significantly upregulated genes (log2FC >2, P<0.05) are shown as black squares, downregulated genes (log2FC <-2, P<0.05) as black triangles and non-significant genes as grey circles. FC, fold change; PTC, papillary thyroid carcinoma.

these 4 genes across the six independent datasets analyzed is illustrated in Fig. 5 as log2FC values, highlighting their consistent dysregulation in PTC. The downregulated genes IQ motif containing GTPase activating protein 3 (*IQGAP3*), mitogen-activated protein kinase 1 (*MAPK1*) and thrombospondin 1 (*THBS1*) were not identified as hub genes based on network centrality and were therefore not selected for RT-qPCR validation.

Verification of hub gene expression by RT-qPCR. To experimentally validate the computational findings, an independent cohort of 86 patients was analyzed. Based on cytological

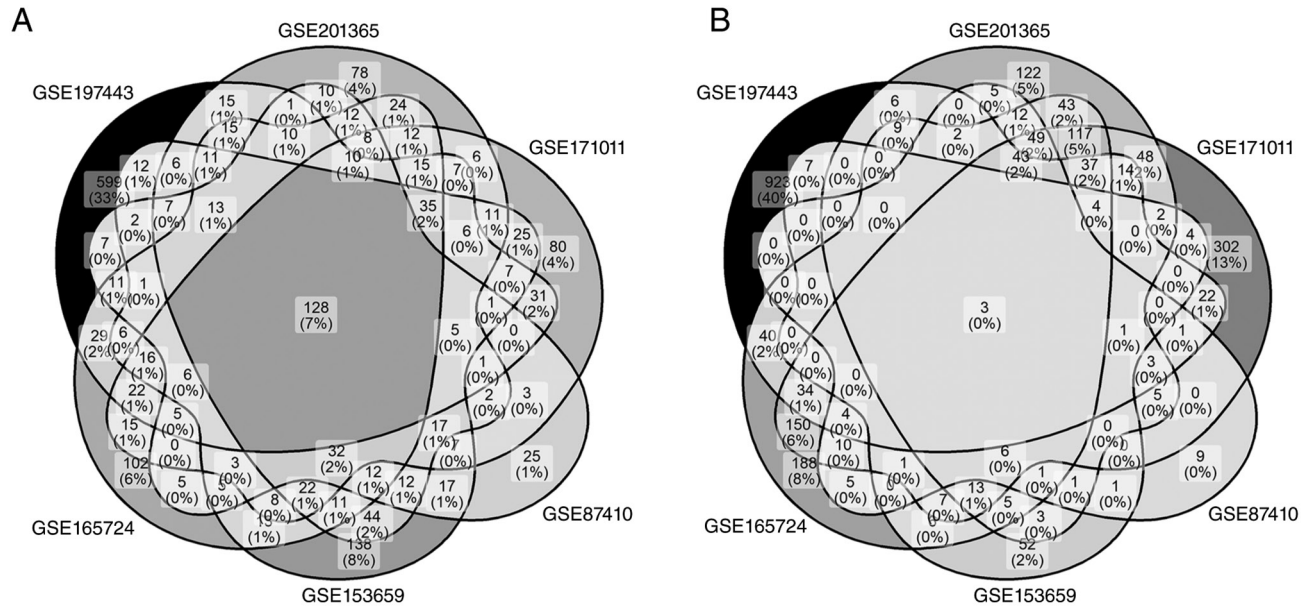

Figure 2. Venn diagram illustrating overlapping dysregulated genes across the six RNA-sequencing datasets. A total of 131 dysregulated common genes were identified, of which (A) 128 were upregulated and (B) 3 were downregulated.

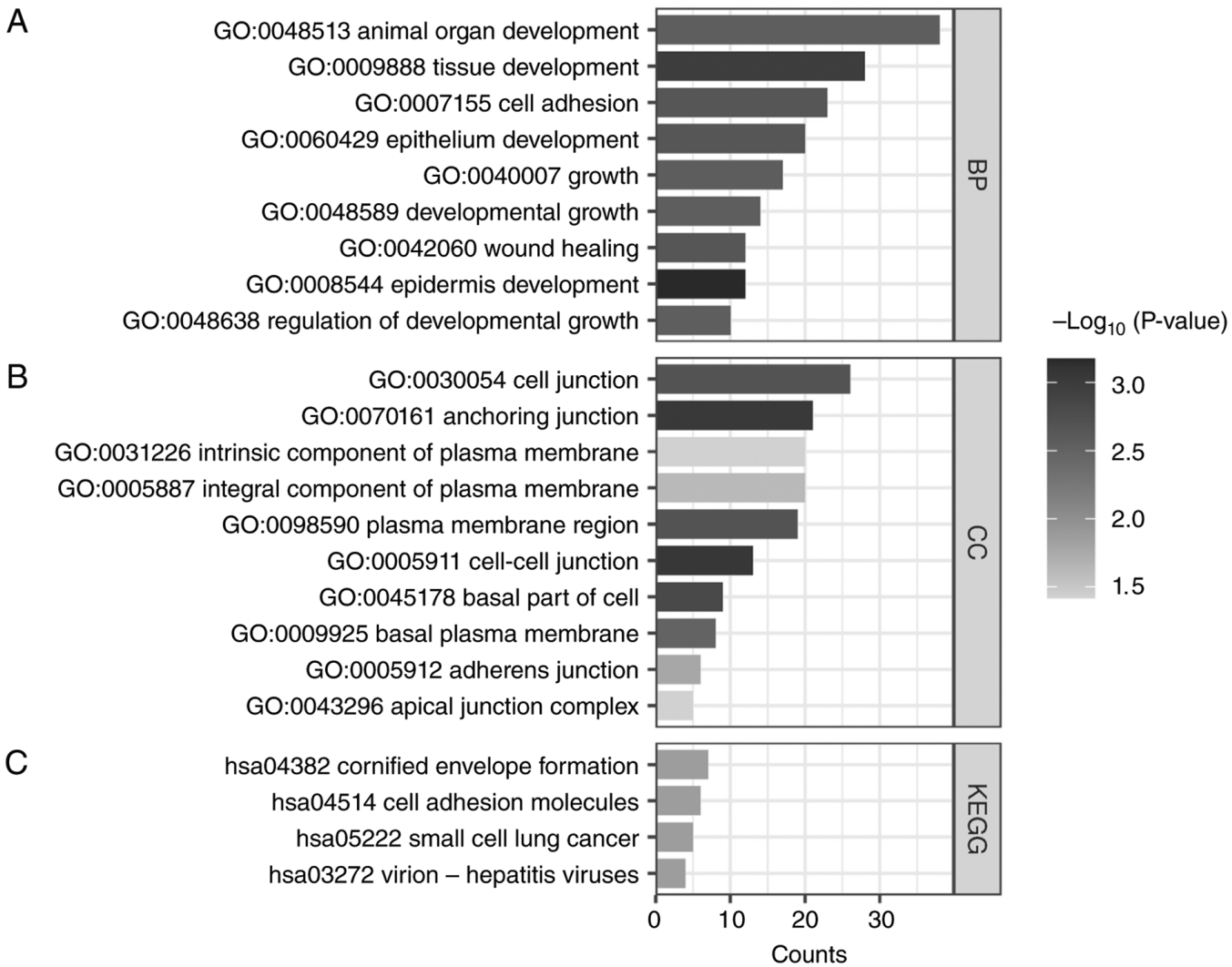

Figure 3. Enriched GO and KEGG terms. Bar plots display the most significantly enriched terms for (A) GO BP, (B) GO CC and (C) KEGG pathways. The x-axis represents the number of differentially expressed genes associated with each term, and the gray scale indicates statistical significance (-$\log_{10}$ P-value). GO, Gene Ontology; KEGG, Kyoto Encyclopedia of Genes and Genomes; BP, biological process; CC, cellular component.

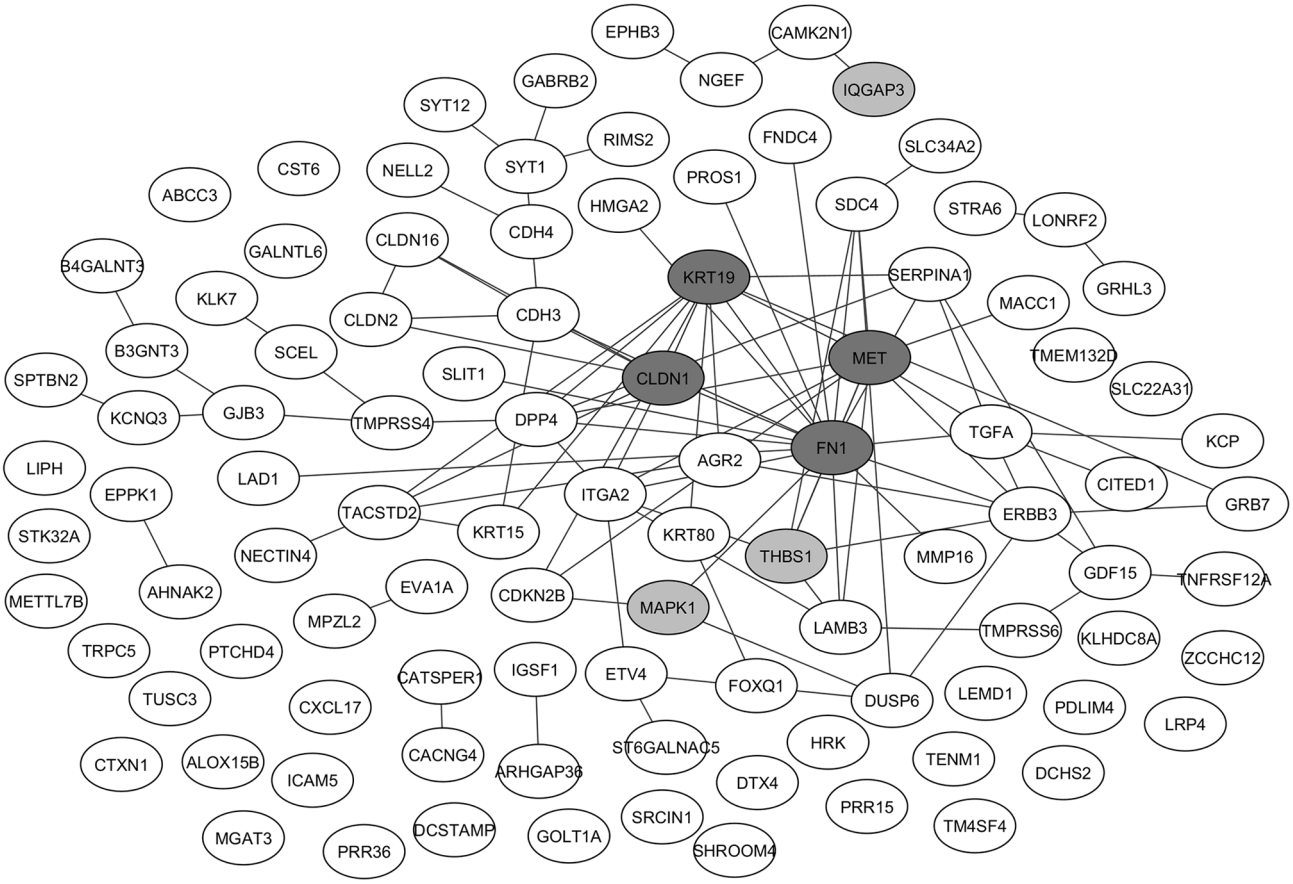

Figure 4. PPI network of dysregulated genes. The PPI network was constructed using the consensus list of 131 DEGs identified across all six datasets. The network was generated using the STRING database (version 12.0) and visualized in Cytoscape (version 3.10.2). Nodes represent proteins encoded by DEGs and edges indicate predicted functional associations. All DEGs were included in the network prior to the application of centrality-based methods for hub gene identification. Downregulated genes (*IQGAP3*, *MAPK1* and *THBS1*) are shown in light gray, while the 4 hub genes identified after centrality analysis (*FN1, MET, KRT19* and *CLDN1*) are shown in dark gray. PPI, protein-protein interaction; DEGs, differentially expressed genes; *IQGAP3*, IQ motif containing GTPase activating protein 3; *MAPK1*, mitogen-activated protein kinase 1; *THBS1*, thrombospondin 1; *FN1*, fibronectin 1; *MET*, MET proto-oncogene receptor tyrosine kinase; *KRT19*, keratin 19; *CLDN1*, claudin 1.

diagnosis according to the Bethesda system, 45 cases were classified as BTN (Bethesda II) and 41 as PTC (Bethesda V-VI). The clinicopathological characteristics of the study cohort are summarized in Table II. No significant differences were observed between the BTN and PTC groups regarding comorbidities, including hypothyroidism, hyperthyroidism, hypertension and diabetes mellitus (all P>0.05).

The mRNA expression levels of the 4 hub genes were quantified by RT-qPCR in all samples. As shown in Fig. 6, all 4 genes displayed significant upregulation in PTC compared with BTN samples (P<0.001). Specifically, the average fold change was 44.50±0.45 for *CLDN1*, 17.46±0.82 for *FN1*, 13.01±0.36 for *KRT19* and 12.67±0.67 for *MET*. These findings from the current independent patient cohort were consistent with the *in silico* results, supporting the consistent upregulation of *CLDN1*, *FN1*, *KRT19* and *MET* as a characteristic molecular signature of PTC.

In silico validation of hub gene expression at the protein level. To further evaluate whether the transcriptomic alterations were reflected at the protein level, representative IHC images were retrieved from the Human Protein Atlas. *CLDN1*, *FN1*, *KRT19* and *MET* exhibited stronger immunoreactivity in PTC tissues than in normal thyroid tissue. Normal thyroid samples showed low or basal staining, whereas tumor tissues displayed increased protein expression (Fig. 7). These observations were consistent with the transcriptomic expression patterns identified in the present study.

Discussion

The present study identified a reproducible set of genes consistently dysregulated in PTC across multiple independent transcriptomic datasets and verified their upregulation in clinically derived thyroid nodule samples. Although alterations in *FN1*, *MET*, *KRT19* and *CLDN1* have been previously reported (8,18,35), variability across independent cohorts has limited the establishment of a stable molecular framework, highlighting the need for cross-dataset validation to distinguish consistently dysregulated genes from dataset-specific findings. In this context, the novelty of the present study lies in the integrative analytical approach, combining multi-dataset RNA-seq analysis with PPI network-based prioritization and experimental validation in an independent cohort of FNA samples. In contrast to previous studies, which are often based on single datasets

Table I. Top 10 hub genes ranked by six different centrality algorithms calculated with the Cytohubba plugin.

Rank	MNC	Degree	Closeness	Radiality	MCC	EPC
1	*FN1*[a]	*FN1*[a]	*FN1*[a]	*FN1*[a]	*FN1*[a]	*FN1*[a]
2	*MET*[a]	*KRT19*[a]	*KRT19*[a]	*MET*[a]	*MET*[a]	*MET*[a]
3	*KRT19*[a]	*MET*[a]	*MET*[a]	*KRT19*[a]	*KRT19*[a]	*KRT19*[a]
4	*CLDN1*[a]	*CLDN1*[a]	*ERBB3*	*DPP4*	*DPP4*	*DPP4*
5	*ITGA2*	*ERBB3*	*CLDN1*[a]	*CLDN1*[a]	*ITGA2*	*ITGA2*
6	*DPP4*	*TGFA*	*DPP4*	*SERPIN1*	*CLDN1*[a]	*ERBB3*
7	*TGFA*	*ITGA2*	*ITGA2*	*ITGA2*	*ERBB3*	*CLDN1*[a]
8	*TACSTD2*	*DPP4*	*SERPIN1*	*ERBB3*	*TGFA*	*SERPIN1*
9	*SERPIN1*	*CDH3*	*CDH3*	*CDH3*	*CDH3*	*TGFA*
10	*CDH3*	*SERPIN1*	*TGFA*	*TGFA*	*SERPIN1*	*CDH3*

[a]The 4 genes selected for experimental validation (*FN1*, *MET*, *KRT19* and *CLDN1*) consistently appear among the highest-ranked candidates across the different methods, robustly identifying them as the most significant hubs in the papillary thyroid carcinoma network. MNC, Maximum Neighborhood Component; MCC, Maximal Clique Centrality; EPC, Edge Percolated Component; *FN1*, fibronectin 1; *MET*, MET proto-oncogene, receptor tyrosine kinase; *KRT19*, keratin 19; *CLDN1*, claudin 1.

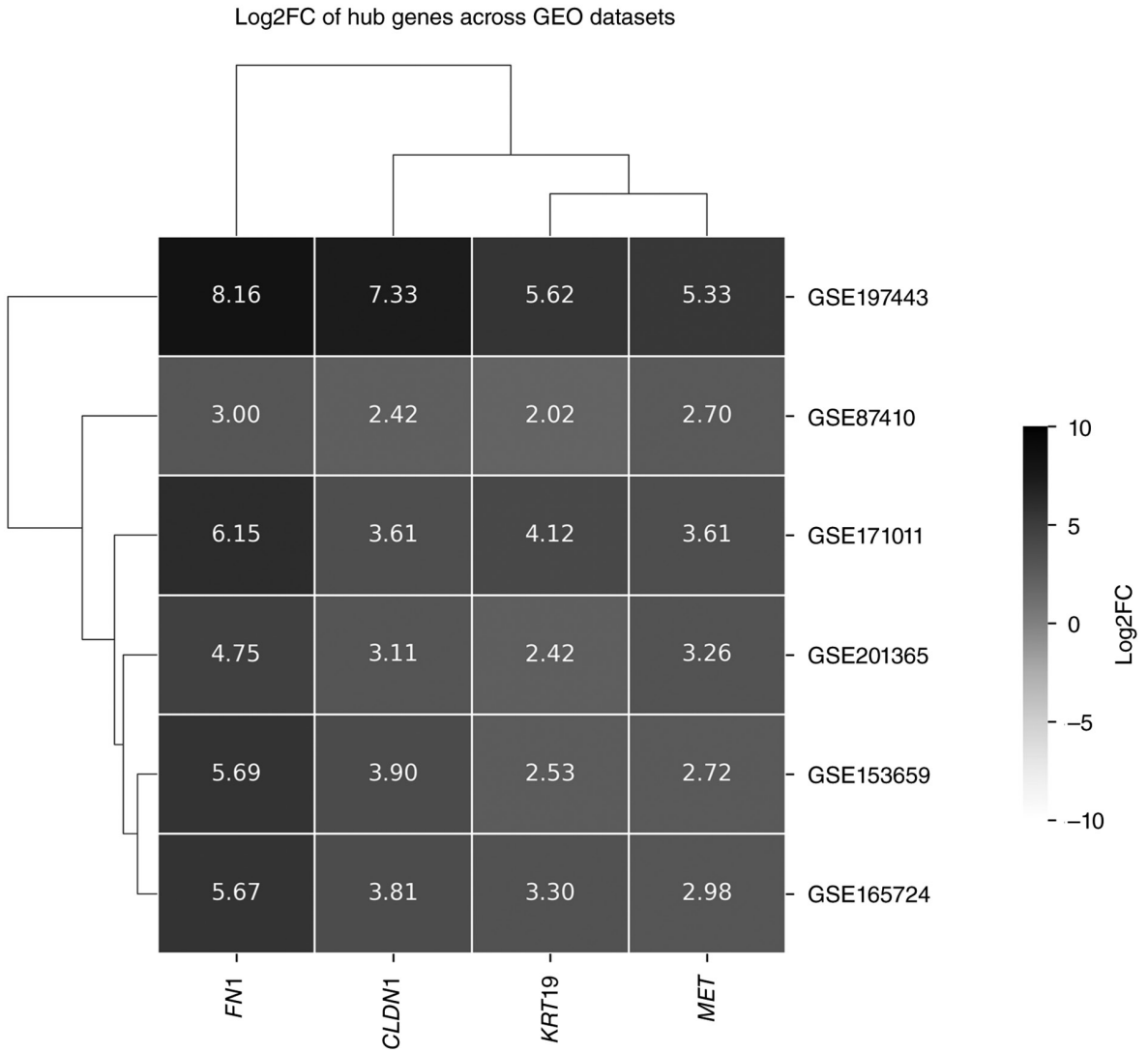

Figure 5. Heatmap of log2FC values for hub genes across the six datasets. Each row corresponds to a Gene Expression Omnibus dataset and each column represents 1 hub gene. The gray scale ranges from -10 (white, downregulation) to +10 (black, upregulation). Across all datasets, the 4 hub genes consistently show positive log2FC values, indicating strong and reproducible upregulation in PTC. *FN1*, fibronectin 1; *MET*, MET proto-oncogene, receptor tyrosine kinase; *KRT19*, keratin 19; *CLDN1*, claudin 1.

Table II. Clinicopathological characteristics of the study cohort.

Variable	BTN (n=45)	PTC (n=41)	Total (n=86)	P-value
Bethesda category, n (%)				<0.001
II	45 (100.0)	0 (0.0)	45 (52.3)	
V	0 (0.0)	6 (14.6)	6 (7.0)	
VI	0 (0.0)	35 (85.4)	35 (40.7)	
Sex, n (%)				0.918
Women	37 (82.2)	35 (85.4)	72 (83.7)	
Men	8 (17.8)	6 (14.6)	14 (16.3)	
Mean age ± SD (range), years	52.6±16.3 (26-83)	45.6±18.5 (14-80)	49.40±17.6	0.071
Hypothyroidism, n (%)				0.174
Yes	6 (13.3)	11 (26.8)	17 (19.8)	
No	39 (86.7)	30 (73.2)	69 (80.2)	
Hyperthyroidism, n (%)				1.000
Yes	0 (0.0)	0 (0.0)	0 (0.0)	
No	45 (100.0)	45 (100.0)	86 (100.0)	
Hypertension, n (%)				0.264
Yes	10 (22.2)	5 (12.2)	15 (17.4)	
No	35 (77.8)	36 (87.8)	71 (82.6)	
Diabetes mellitus, n (%)				0.187
Yes	1 (2.2)	4 (9.8)	5 (5.8)	
No	44 (97.8)	37 (90.2)	81 (94.2)	

PTC, papillary thyroid carcinoma; BTN, benign thyroid nodule.

or limited microarray platforms, the present study focused on genes consistently dysregulated across independent cohorts. Earlier studies relying on individual GEO datasets or small sample sizes (7,9,10) may introduce cohort-specific variability and have reported considerable differences in the number and identity of DEGs. In addition, candidate genes are frequently selected based solely on differential expression, without evaluating reproducibility across datasets or incorporating robust network-level prioritization. Although some studies include PPI analyses, these are often limited to basic network construction without applying multiple centrality measures (16,17). By integrating six independent RNA-seq cohorts, the present study enhanced the robustness and reproducibility of gene identification. The inclusion of network-based prioritization using multiple centrality algorithms, together with validation in an independent FNA cohort, provided a more robust and translational framework, identifying genes that are not only consistently dysregulated but also biologically and clinically relevant in PTC.

Notably, in the present study, the validation of *FN1*, *MET*, *KRT19* and *CLDN1* in a Mexican Mestizo population, in comparison with datasets derived from different populations, supports their cross-population consistency and suggests that the alterations in the expression of these genes are not population-specific. This aspect strengthens their potential applicability in diverse clinical settings and reinforces their relevance as stable molecular features of PTC. Collectively, these findings support the presence of a consistent transcriptomic pattern in PTC.

The intersection-based strategy, combined with the stringent |log2FC|>2 threshold, likely resulted in a conservative gene set, particularly refining the number of commonly dysregulated genes identified. However, this approach was intentionally adopted to prioritize robustness and cross-dataset reproducibility, ensuring that the identified genes represent consistent transcriptional alterations rather than dataset-specific effects.

In the present study, 3 genes (*IQGAP3*, *MAPK1* and *THBS1*) were consistently identified as being downregulated; however, they were not prioritized for further analysis due to their lower centrality within the PPI network. Functionally, IQGAP3 is involved in cytoskeletal organization and cell proliferation (36), MAPK1 participates in MAPK/extracellular signal-regulated kinase (ERK) signaling pathways that regulate cell growth and differentiation (37) and THBS1 is associated with extracellular matrix interactions, angiogenesis and the regulation of cell proliferation and apoptosis (38), suggesting a more peripheral role within the interaction network identified in the present study.

Among the consistently upregulated genes identified, *FN1* emerged as a central component of the interaction network. *FN1* encodes fibronectin, an extracellular matrix glycoprotein that mediates cell-matrix adhesion and contributes to tissue stiffness (35,39). In PTC, its upregulation activates signaling pathways that promote cell migration and invasion and has been associated with activation of vascular endothelial growth factor-related signaling, thereby increasing the risk of lymph node metastasis (40). FN1 contributes to extracellular matrix

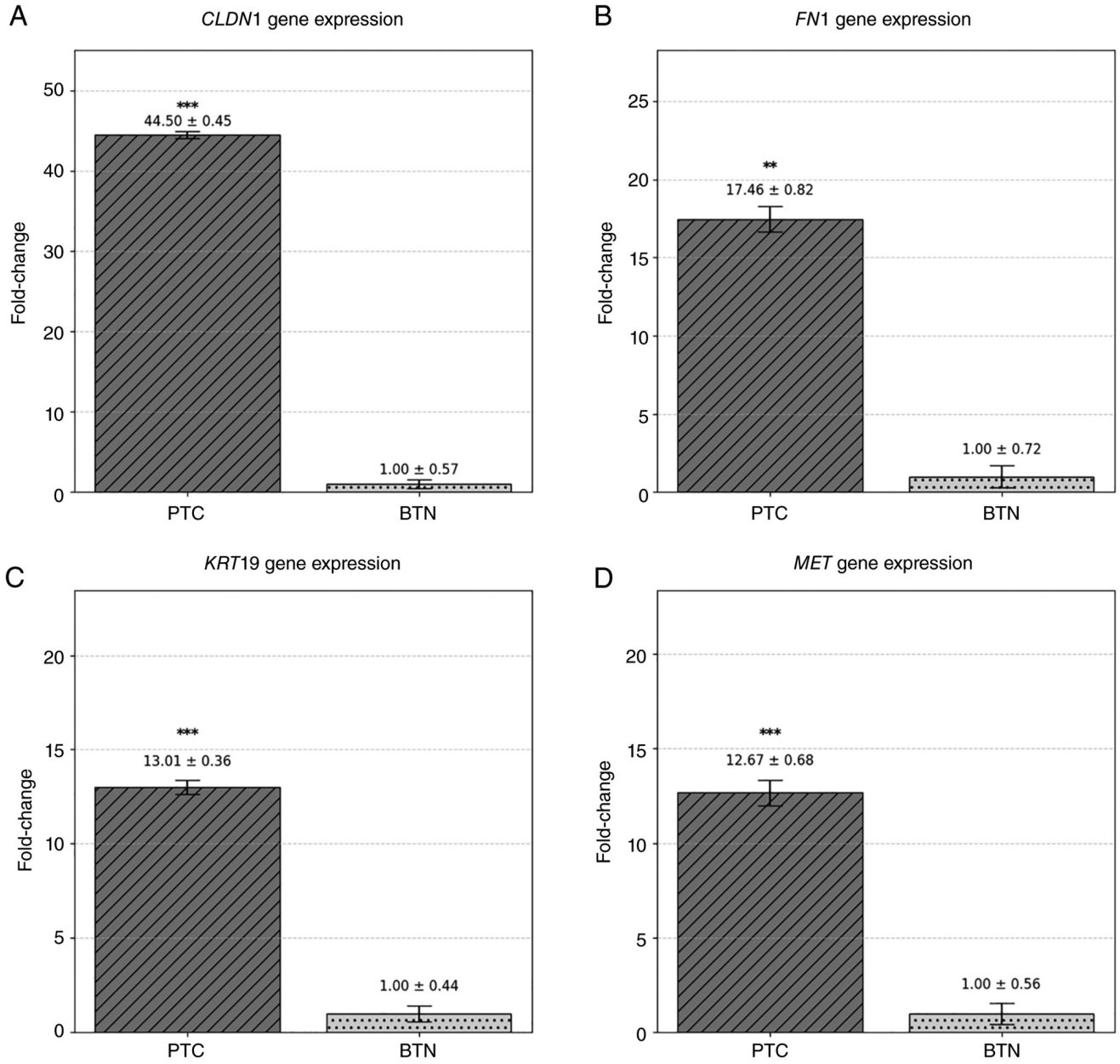

Figure 6. Relative mRNA expression of hub genes in PTC. Bar charts showing the fold change in expression for (A) *CLDN1*, (B) *FN1*, (C) *KRT19* and (D) *MET* in PTC tissues compared with that in BTN tissues. Expression levels in the BTN group were normalized to 1 using b-actin as the reference gene. All 4 genes show significant upregulation in the PTC samples. Bars represents fold change ± standard deviation. **P<0.01 and ***P<0.001 vs. BTN. PTC, papillary thyroid carcinoma; BTN, benign thyroid nodule; *FN1*, fibronectin 1; *MET*, MET proto-oncogene, receptor tyrosine kinase; *KRT19*, keratin 19; *CLDN1*, claudin 1.

remodeling and cell-matrix adhesion and interacts with integrin receptors, activating downstream signaling pathways such as focal adhesion kinase, phosphatidylinositol 3-kinase/protein kinase B (PI3K/AKT) and MAPK/ERK, which are associated with proliferation, survival and migration (41). In addition, *FN1* expression has been reported to be regulated by pathways such as TGF-β signaling, linking extracellular matrix remodeling with epithelial plasticity in thyroid cancer (42). *FN1* upregulation has been associated with aggressive clinicopathological features, including lymph node metastasis and extrathyroidal extension. Mechanistically, FN1-integrin interactions, particularly involving αv-containing integrins, have been shown to promote tumor cell proliferation and migration, supporting a functional role for FN1 in PTC progression (43).

MET encodes the hepatocyte growth factor receptor c-Met, a receptor tyrosine kinase activated by hepatocyte growth factor that transduces proliferative, migratory and angiogenic signals (44,45) triggering signaling cascades, including PI3K/AKT and MAPK/ERK, that promote proliferation, survival and invasive behavior (46). *MET* activation has been shown to enhance tumor cell proliferation and migration through ERK and PI3K/AKT signaling pathways, and to cooperate with integrin-mediated mechanisms, further supporting its role in PTC progression (47).

Previous studies have shown that *MET* upregulation in PTC may be associated with the *BRAFV600E* mutation and a more aggressive phenotype, thus facilitating local invasion and lymphatic spread (45,48).

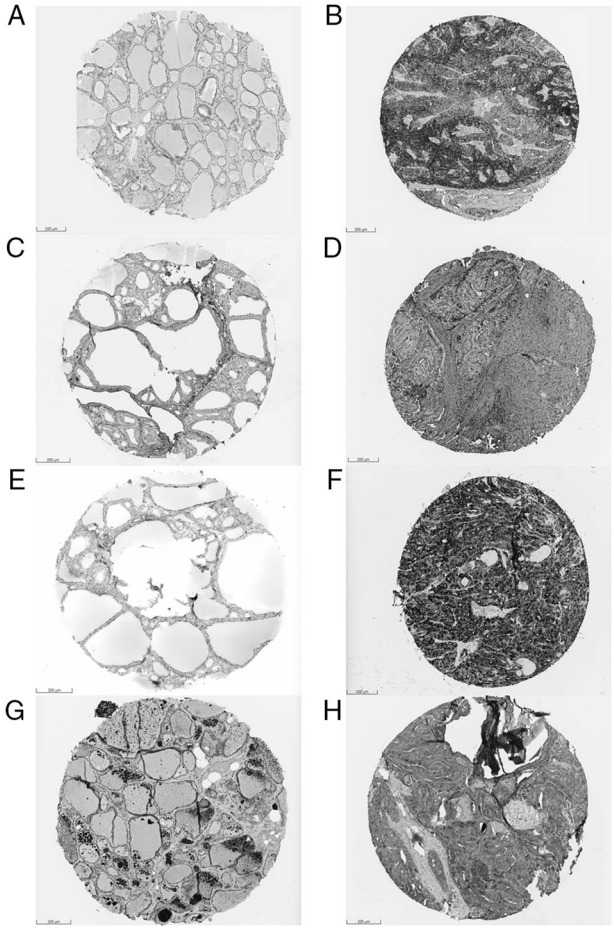

Figure 7. Immunohistochemical expression patterns of key proteins in normal thyroid and PTC tissues. Panels on the left represent normal thyroid gland tissue, whereas panels on the right show PTC tissue. Specific protein staining is as follows: (A and B) CLDN1 (antibody CAB002602), (C and D) FN1 (antibody CAB000126), (E and F) KRT19 (antibody CAB00031) and (G and H) MET (antibody CAB005282). Images show stronger immunoreactivity in PTC compared with normal thyroid tissue. Images were obtained from the Human Protein Atlas database (https://www.proteinatlas.org). Scale bars, 200 μm. PTC, papillary thyroid carcinoma.

KRT19 encodes a 40-kDa type I acidic keratin protein, an intermediate filament protein that forms part of the cytoskeletal scaffolding within epithelial cells, and thus is involved in maintaining epithelial cell architecture and mechanical stability and contributes to the structural integrity and organization of epithelial cells (49). *KRT19* upregulation has been consistently reported in PTC and is associated with lymph node metastasis and advanced tumor stage. Mechanistically, KRT19 has been shown to promote tumor cell proliferation and migration through epithelial-mesenchymal transition-related processes, supporting its role in PTC progression (50).

These epithelial-mesenchymal transition-related processes are functionally interconnected through extracellular matrix-receptor interactions, junctional dynamics and growth factor signaling pathways, which collectively regulate tumor cell proliferation, invasion and epithelial plasticity in PTC. The coordinated dysregulation of these extracellular, junctional, cytoskeletal and signaling components suggests remodeling of epithelial architecture characterized by altered adhesion dynamics, structural reorganization and enhanced migratory capacity, consistent with mechanisms underlying PTC progression.

CLDN1 encodes claudin-1, a tight junction protein that plays a key role in maintaining intercellular adhesion and regulates epithelial barrier integrity and polarity (51). Dysregulation of claudins can compromise epithelial barrier integrity and promote tumor invasion (52). A previous study demonstrated that *CLDN1* overexpression in thyroid cells can enhance cellular migration and invasiveness (52). *CLDN1* upregulation has been reported and is associated with aggressive clinicopathological features, including lymph node metastasis and invasive behavior in PTC (53,54). Mechanistically, CLDN1 has been linked to epithelial-mesenchymal transition-related processes and activation of pathways such as TGF-β signaling, promoting tumor cell proliferation, migration and invasion. In addition, *CLDN1* dysregulation has been associated with modulation of the tumor immune microenvironment, including reduced $CD8^+$ T cell infiltration, further supporting its role in PTC progression (54).

Several of the aforementioned hub genes have been previously reported in other studies on PTC. A study that aimed to elucidate the molecular mechanisms underlying PTC and to identify potential biomarkers and therapeutic targets using microarray data, identified 8 genes, including *KRT19*, *FN1* and *MET* (8). Another investigation conducted in 2018 analyzed both public databases and institutional samples to identify key genes and microRNAs (miRNAs/miRs) associated with PTC progression, tumor stage and prognosis (18). In that study, miR-204-5p was identified as an important regulatory miRNA that could negatively regulate target genes such as *FN1* and *CLDN1*, which were associated with tumor stage and prognosis, respectively. Notably, gene expression validation was performed in PTC samples and matched normal peritumoral tissues using RT-qPCR, verifying the upregulation of these genes.

Particularly, *FN1* has been consistently reported to exhibit increased expression in PTC, consistent with the results of the present study. However, those investigations were limited to *in silico* validation based on publicly available datasets such as TCGA and GEPIA (11,12,17). Similarly, another study identified *KRT19* and *FN1* as highly connected genes, with further analysis focusing on *FN1* due to its highest centrality value (35). In addition, IHC data from the Human Protein Atlas analyzed in that study also confirmed significantly elevated protein expression levels of FN1 and KRT19 in PTC tissues. Furthermore, increased *FN1* expression was strongly associated with advanced pathological stage, higher tumor grade and enhanced immune cell infiltration. In the present study, *FN1* expression displayed a 17-fold increase in PTC compared with BTN. Previous studies have similarly reported marked *FN1* overexpression in PTC, although the magnitude of the reported fold change varies across studies. For example, a study reported a 120-fold increase in *FN1* expression in nine PTC samples and paired peritumoral normal thyroid tissues using GAPDH as the reference gene (18). The higher fold change observed in that study may reflect differences in the comparison group (adjacent normal thyroid tissue vs. BTN), sample size and normalization strategy. Consistently, a TCGA analysis revealed ~5,000 *FN1* transcripts per million (TPM) in classical PTC samples (n=358), compared with a markedly

lower *FN1* expression level of ~0 TPM in normal thyroid tissue (n=59) (11). Another TCGA-based study reported a 12-fold increase in *FN1* expression in PTC compared with that in normal thyroid tissue (12). In another investigation analyzing 103 paired PTC tissue samples, a 4-fold increase in *FN1* in PTC compared with normal thyroid tissues was observed (35).

Regarding *MET*, the results of the present study demonstrated a 12-fold increase in expression in PTC samples relative to that in BTN samples. A previous study examining the role of miR-3666 in the pathogenesis of PTC revealed an inverse association between miR-3666 and *MET* expression in tumor samples from 25 patients, analyzed by RT-qPCR, where downregulation of miR-3666 coincided with *MET* upregulation (44). Further experiments using cell culture models showed that enhanced miR-3666 expression inhibited cell growth and proliferation. Furthermore, bioinformatics analysis indicated that the 3'-untranslated region of *MET* mRNA was a target of miR-3666, thus suggesting that this miRNA could suppress *MET* expression by inhibiting its translation. Another study analyzing PTC tissues from 93 patients, alongside histopathologically confirmed normal thyroid tissues from 9 patients, also reported significantly elevated *MET* expression in PTC, which was associated with an invasive phenotype and lymphatic metastasis (45).

The upregulation of *KRT19* and *CLDN1* has also been previously reported in a cohort of 97 FNA samples (55). The study described fold changes comparable to those observed in the present study. Specifically, *KRT19* expression was found to be 11-fold higher and *CLDN1* 41-fold higher in PTC, while in the present study, *KRT19* expression increased by ~13-fold and *CLDN1* by 44-fold compared with that in BTN. In another study analyzing 5 paired PTC tissue samples, *CLDN1* relative expression was likewise elevated and associated with patient prognosis (18).

A number of limitations should be considered when interpreting the findings of the present study. The classification of thyroid nodules was based on ultrasound-guided FNA cytology according to the Bethesda System, without histopathological confirmation. Although Bethesda categories II, V and VI are widely used in clinical practice and are associated with low and high risks of malignancy, respectively, cytological evaluation does not provide the same level of diagnostic certainty as surgical histopathology. This approach reflects real-world clinical practice, where cytological classification is routinely used to guide management decisions. Therefore, a residual risk of misclassification, including potential false-positive or false-negative cases, cannot be completely excluded. However, to reduce this limitation, only cases with clearly defined cytological categories were included, and all evaluations were performed by a single experienced pathologist. Furthermore, the present study focused on the identification and experimental validation of reproducible hub genes rather than on the development of integrated diagnostic signatures. While combinatorial gene expression models may enhance diagnostic performance in clinical settings, this represents a limitation of the present study, as such approaches were not evaluated. Therefore, the findings reported within the present study provide a foundation for future studies aimed at assessing these strategies in larger and independently validated cohorts. Further studies, including well-characterized cohorts with histopathological confirmation and comprehensive clinical data are required to validate these findings and to further explore their potential clinical applicability.

Collectively, the findings of the present study support the consistent dysregulation of *FN1*, *MET*, *KRT19* and *CLDN1* in PTC across independent datasets and in clinically derived samples. Rather than establishing causative roles, the results of the present study identified these genes as robust candidate markers associated with epithelial remodeling and adhesion-related processes in PTC. Overall, the present integrative transcriptomic expands the current understanding of molecular alterations in PTC for future functional and prospective clinical studies aimed at evaluating their diagnostic and biological significance.

Acknowledgements

Not applicable.

Funding

This study was supported by Sociedad Mexicana de Nutrición y Endocrinología and Universidad Politécnica de Sinaloa.

Availability of data and materials

The data generated in the present study may be requested from the corresponding author.

Authors' contributions

ARGQ and NGM conceived and designed the present study, analyzed data and edited the manuscript, and performed experiments, statistical analysis and original draft preparation. ARO performed experiments and manuscript review and editing. KLMH performed experiments. MAA, DCP, VGF and FLO contributed to the methodology, validation of the analytical framework and interpretation of the data. NGM, MAA and EAM contributed to study conception and overall supervision, secured funding support, and critically revised the manuscript. ARGQ, NGM, ARO, MAA, FLO, KLHM, DCP, VGF and EAM confirm the authenticity of all the raw data. All authors have read and approved the final manuscript.

Ethics approval and consent to participate

All patients signed informed consent forms prior to sample collection. Participants consented to the collection and use of their clinical information and FNA biopsy specimens for research purposes. The informed consent forms and study protocol were reviewed and approved by the Polytechnic University of Sinaloa Ethics and Research Committee (Mazatlán, México; approval no. 001-2022-CEI).

Patient consent for publication

Not applicable.

Competing interests

The authors declare that they have no competing interests.

References

1. Forma A, Kłodnicka K, Pająk W, Flieger J, Teresińska B, Januszewski J and Baj J: Thyroid cancer: Epidemiology, classification, risk factors, diagnostic and prognostic markers, and current treatment strategies. Int J Mol Sci 26: 5173, 2025.
2. Pusztaszeri MP, Auger M, Stelow EB, Yang GCH, Sanchez MA and LiVolsi VA: Papillary Thyroid Carcinoma, Variants, and Related Tumors. In: The Bethesda System for Reporting Thyroid Cytopathology. Ali SZ and Cibas ES (eds.): Springer International Publishing, Cham, pp119-156, 2018.
3. Abdullah MI, Junit SM, Ng KL, Jayapalan JJ, Karikalan B and Hashim OH: Papillary thyroid cancer: Genetic alterations and molecular biomarker investigations. Int J Med Sci 16: 450-460, 2019.
4. Metovic J, Cabutti F, Osella-Abate S, Orlando G, Tampieri C, Napoli F, Maletta F, Daniele L, Volante M and Papotti M: Clinical and pathological features and gene expression profiles of clinically aggressive papillary thyroid carcinomas. Endocr Pathol 34: 298-310, 2023.
5. Ringel MD, Sosa JA, Baloch Z, Bischoff L, Bloom G, Brent GA, Brock PL, Chou R, Flavell RR, Goldner W, *et al*: 2025 American thyroid association management guidelines for adult patients with differentiated thyroid cancer. Thyroid 35: 841-985, 2025.
6. Tsakiroglou M, Evans A and Pirmohamed M: Leveraging transcriptomics for precision diagnosis: Lessons learned from cancer and sepsis. Front Genet 14: 1100352, 2023.
7. Zhu W, Li C and Ai Z: Candidate agents for papillary thyroid cancer identified by gene expression analysis. Pathol Oncol Res 19: 597-604, 2013.
8. Qu T, Li YP, Li XH and Chen Y: Identification of potential biomarkers and drugs for papillary thyroid cancer based on gene expression profile analysis. Mol Med Rep 14: 5041-5048, 2016.
9. Yu J, Mai W, Cui Y and Kong L: Key genes and pathways predicted in papillary thyroid carcinoma based on bioinformatics analysis. J Endocrinol Invest 39: 1285-1293, 2016.
10. Ao Z, Chen Y, Lu JM, Shen J, Peng LP, Lin X, Peng C, Zeng CP, Wang XF, Zhou R, *et al*: Identification of potential functional genes in papillary thyroid cancer by co-expression network analysis. Oncol Lett 16: 4871-4878, 2018.
11. Zhang S, Wang Q, Han Q, Han H and Lu P: Identification and analysis of genes associated with papillary thyroid carcinoma by bioinformatics methods. Biosci Rep 39: BSR20190083, 2019.
12. Shen Y, Dong S, Liu J, Zhang L, Zhang J, Zhou H and Dong W: Identification of potential biomarkers for thyroid cancer using bioinformatics strategy: A study based on GEO datasets. BioMed Res Int 2020: 9710421, 2020.
13. Liu Y, Gao S, Jin Y, Yang Y, Tai J, Wang S, Yang H, Chu P, Han S, Lu J, *et al*: Bioinformatics analysis to screen key genes in papillary thyroid carcinoma. Oncol Lett 19: 195-204, 2019.
14. Fan R, Dong L, Li P, Wang X and Chen X: Integrated bioinformatics analysis and screening of hub genes in papillary thyroid carcinoma. PLoS One 16: e0251962, 2021.
15. Liao M, Wang Z, Yao J, Xing H, Hao Y and Qiu B: Identification of potential biomarkers for papillary thyroid carcinoma by comprehensive bioinformatics analysis. Mol Cell Biochem 478: 2111-2123, 2023.
16. Han J, Chen M, Wang Y, Gong B, Zhuang T, Liang L and Qiao H: Identification of biomarkers based on differentially expressed genes in papillary thyroid carcinoma. Sci Rep 8: 9912, 2018.
17. Xue G, Lin X, Wu JF, Pei D, Wang DM, Zhang J and Zhang WJ: Identification of key genes of papillary thyroid carcinoma by integrated bioinformatics analysis. Biosci Rep 40: BSR20201555, 2020.
18. Qiu J, Zhang W, Zang C, Liu X, Liu F, Ge R, Sun Y and Xia Q: Identification of key genes and miRNAs markers of papillary thyroid cancer. Biol Res 51: 45, 2018.
19. Barrett T, Wilhite SE, Ledoux P, Evangelista C, Kim IF, Tomashevsky M, Marshall KA, Phillippy KH, Sherman PM, Holko M, *et al*: NCBI GEO: Archive for functional genomics data sets-update. Nucleic Acids Res 41: D991-D995, 2012.
20. Liu L, Zhao Q, Cheng C, Yi J, Sun H, Wang Q, Quan W, Xue Y, Sun L, Cong X and Zhang Y: Analysis of bulk RNA sequencing data reveals novel transcription factors associated with immune infiltration among multiple cancers. Front Immunol 12: 644350, 2021.
21. Yang F, Lian M, Ma H, Feng L, Shen X, Chen J and Fang J: Identification of key genes associated with papillary thyroid microcarcinoma characteristics by integrating transcriptome sequencing and weighted gene co-expression network analysis. Gene 811: 146086, 2022.
22. Lv C, Sun W, Huang J, Qin Y, Ji X and Zhang H: Expression profiles of circular RNAs in human papillary thyroid carcinoma based on RNA deep sequencing. Onco Targets Ther 14: 3821-3832, 2021.
23. Hu H, Chen Q, Zheng S, Du S, Ding S and Lun Y: Transcriptome analysis revealed potential Neuro-Immune interaction in papillary thyroid carcinoma tissues. Diseases 11: 9, 2023.
24. He H, Liyanarachchi S, Li W, Comiskey DF Jr, Yan P, Bundschuh R, Turkoglu AM, Brock P, Ringel MD and de la Chapelle A: Transcriptome analysis discloses dysregulated genes in normal appearing tumor-adjacent thyroid tissues from patients with papillary thyroid carcinoma. Sci Rep 11: 14126, 2021.
25. Love MI, Huber W and Anders S: Moderated estimation of fold change and dispersion for RNA-seq data with DESeq2. Genome Biol 15: 550, 2014.
26. Kanehisa M: KEGG: Kyoto encyclopedia of genes and genomes. Nucleic Acids Res 28: 27-30, 2000.
27. Ashburner M, Ball CA, Blake JA, Botstein D, Butler H, Cherry JM, Davis AP, Dolinski K, Dwight SS, Eppig JT, *et al*: Gene ontology: Tool for the unification of biology. Nat Genet 25: 25-29, 2000.
28. Yu G, Wang LG, Han Y and He QY: clusterProfiler: An R package for comparing biological themes among gene clusters. OMICS 16: 284-287, 2012.
29. Szklarczyk D, Nastou K, Koutrouli M, Kirsch R, Mehryary F, Hachilif R, Hu D, Peluso ME, Huang Q, Fang T, *et al*: The STRING database in 2025: Protein networks with directionality of regulation. Nucleic Acids Res 53: D730-D737, 2025.
30. Shannon P, Markiel A, Ozier O, Baliga NS, Wang JT, Ramage D, Amin N, Schwikowski B and Ideker T: Cytoscape: A software environment for integrated models of biomolecular interaction networks. Genome Res 13: 2498-2504, 2003.
31. Chin CH, Chen SH, Wu HH, Ho CW, Ko MT and Lin CY: cytoHubba: Identifying hub objects and sub-networks from complex interactome. BMC Syst Biol 8 (Suppl 4): S11, 2014.
32. Cibas ES and Ali SZ: The 2017 Bethesda system for reporting thyroid cytopathology. Thyroid 27: 1341-1346, 2017.
33. Livak KJ and Schmittgen TD: Analysis of relative gene expression data using real-time quantitative PCR and the 2(-Delta Delta C(T)) method. Methods 25: 402-408, 2001.
34. Thul PJ and Lindskog C: The human protein atlas: A spatial map of the human proteome. Protein Sci 27: 233-244, 2018.
35. Pan H, Luo Z, Lin F, Zhang J, Xiong T, Hong Y, Sun B and Yang Y: FN1, a reliable prognostic biomarker for thyroid cancer, is associated with tumor immunity and an unfavorable prognosis. Oncol Lett 28: 510, 2024.
36. Wei T and Lambert PF: Role of IQGAP1 in carcinogenesis. Cancers (Basel) 13: 3940, 2021.
37. Wang J, Yang H, Si Y, Hu D, Yu Y, Zhang Y, Gao M and Zhang H: Iodine promotes tumorigenesis of thyroid cancer by suppressing Mir-422a and Up-Regulating MAPK1. Cell Physiol Biochem 43: 1325-1336, 2017.
38. Li Z, He T, Xing Z, Zhu J, Wu W and Su A: Inhibition of THBS1 axis contributes to the antitumor effect of PA-MSHA in anaplastic thyroid cancer. Exp Cell Res 444: 114373, 2025.
39. Zhang M and Zhang B: Extracellular matrix stiffness: Mechanisms in tumor progression and therapeutic potential in cancer. Exp Hematol Oncol 14: 54, 2025.
40. Liu M, Chen P, Wei B, Tan HL, Zhao YX, Ai L, Li N, Jiang YK, Lin J, Li SJ and Chang S: FN1 shapes the behavior of papillary thyroid carcinoma through alternative splicing of EDB region. Sci Rep 15: 327, 2025.
41. Ashok G, Miryala SK, Saju MT, Anbarasu A and Ramaiah S: FN1 encoding fibronectin as a pivotal signaling gene for therapeutic intervention against pancreatic cancer. Mol Genet Genomics 297: 1565-1580, 2022.
42. Udinotti M, Siebolts U, Bauer M, Vaxevanis C, Asiminas A, Lorenz K, Dierks C, Wickenhauser C and Seliger B: Fibroblast activation protein (FAP)-mediated promotion of metastasis via the FN1-TGFβ axis and immune suppression in aggressive thyroid cancer. J Transl Med 23: 1284, 2025.
43. Rocco D, Tortora A, Marotta V, Machado AM, Selistre-de-Araújo HS and Vitale M: Integrin-fibronectin interaction is a pivotal biological and clinical determinant in papillary thyroid carcinoma. Endocr Relat Cancer 32: e250101, 2025.
44. Bu R, Uddin S, Ahmed M, Hussain AR, Alsobhi S, Amin T, Al-Nuaim A, Al-Dayel F, Abubaker J, Bavi P and Al-Kuraya KS: c-Met inhibitor synergizes with tumor necrosis Factor-Related Apoptosis-induced ligand to induce papillary thyroid carcinoma cell death. Mol Med 18: 167-177, 2012.

45. Johansson K, Stenman A, Paulsson JO, Wang N, Ihre-Lundgren C, Zedenius J and Juhlin CC: Development of metastatic poorly differentiated thyroid cancer from a sub-centimeter papillary thyroid carcinoma in a young patient with a germline MET mutation-association or random chance? Thyroid Res 14: 19, 2021.
46. Pothula SP, Xu Z, Goldstein D, Pirola RC, Wilson JS and Apte MV: Targeting HGF/c-MET Axis in Pancreatic Cancer. Int J Mol Sci 21: 9170, 2020.
47. Lan Y, Liu D, Liang B, Song X, Xie L, Peng H, Guo H, Hong C, Weng X, Wei X, *et al*: ITGA3-MET interaction promotes papillary thyroid cancer progression via ERK and PI3K/AKT pathways. Ann Med 57: 2483379, 2025.
48. Chen BK, Ohtsuki Y, Furihata M, Takeuchi T, Iwata J, Liang SB and Sonobe H: Overexpression of c-Met protein in human thyroid tumors correlated with lymph node metastasis and clinicopathologic stage. Pathol Res Pract 195: 427-433, 1999.
49. Menz A, Bauer R, Kluth M, Marie von Bargen C, Gorbokon N, Viehweger F, Lennartz M, Völkl C, Fraune C, Uhlig R, *et al*: Diagnostic and prognostic impact of cytokeratin 19 expression analysis in human tumors: A tissue microarray study of 13,172 tumors. Hum Pathol 115: 19-36, 2021.
50. Wang X, Xu X, Peng C, Qin Y, Gao T, Jing J and Zhao H: BRAFV600E-induced KRT19 expression in thyroid cancer promotes lymph node metastasis via EMT. Oncol Lett 18: 927-935, 2019.
51. Bhat AA, Syed N, Therachiyil L, Nisar S, Hashem S, Macha MA, Yadav SK, Krishnankutty R, Muralitharan S, Al-Naemi H, *et al*: Claudin-1, A double-edged sword in cancer. Int J Mol Sci 21: 569, 2020.
52. Borowczak J, Łaszczych D, Olejnik K, Michalski J, Gutowska A, Kula M, Bator A, Sekielska-Domanowska M, Makarewicz R, Marszałek A, *et al*: Tight junctions and cancer: Targeting Claudin-1 and Claudin-4 in thyroid pathologies. Pharmaceuticals 17: 1304, 2024.
53. Ross-Orozco A, Gastelum-Quiroz AR, Alvarez-Arrazola M, Luque-Ortega F, Martínez-Camberos A, Morales-Hernandez K, Lopez-Herrera Y Cairo F and García-Magallanes N: Association between BRAFV600E mutation and gene expression of CLDN1, TIMP1, and KRT19 in papillary thyroid cancer. Mol Cell Endocrinol 607: 112614, 2025.
54. Wu J, Wang Y, Yan L and Dong Y: Expression of CLDN1 and EGFR in PTC. Discov Oncol 15: 562, 2024.
55. Martínez-Camberos A, Alvarez-Arrazola M, Arámbula-Meraz E, Romero-Quintana J, Luque-Ortega F, Romo-Martinez E, Sánchez-Urbina R, Cedano-Prieto D, González-Castillo A and García-Magallanes N: Dysregulation of KRT19, TIMP1, and CLDN1 gene expression is associated with thyroid cancer. Biochem Biophys Res Commun 617: 55-59, 2022.